High air flotation efficiency of multiphase flow pump with the addition of dodecyl dimethyl benzyl ammonium chloride (DDBAC)

Huan Liu, Wande Ding and Kefeng Zhang

ABSTRACT

Recently, centrifugal multiphase pump–dissolved air flotation (CMP-DAF) has become an increasingly popular alternative to DAF that can achieve more stable performance and higher removal efficiency, and this method is widely used in sewage treatment. However, the nonuniformity of the bubble size and low adherence of the floc particles and bubbles, as well as the complicated raw water quality, pose great challenges to CMP-DAF, which does not meet the standards of water supply and drainage in practical use. In the present study, the surfactant dodecyl dimethyl benzyl ammonium chloride (DDBAC) was utilized as a flotation agent to further improve the flotation efficiency of the CMP-DAF process. DDBAC at a dosage of 0.2 mg/L was introduced to the air flotation of raw water to construct a flotation enhanced CMP air flotation system. The results showed that the average turbidity decreased to 0.433 ± 0.017 NTU, and effluent floc particles were present at 1,053 cnt/mL with an acceptable removal rate of 96.20%. In addition, 34.0% and 30.1% of UV_{254} and COD_{Mn} were removed, respectively. These results imply that DDBAC can increase the collision efficiency of bubble particles by reducing the diameter of the bubbles, which is conducive to forming larger flocs, and enhancing the shear resistance of the bubble–floc particles, thus improving the air flotation efficiency.

Key words | bubble size, centrifugal multiphase pump, drinking water, flotation, water purification

Huan Liu[†]
Wande Ding[†]
Kefeng Zhang (corresponding author)
School of Municipal and Environmental Engineering,
Shandong Jianzhu University,
Jinan 250101,
China
E-mail: *kfz@sdjzu.edu.cn*

[†]Huan Liu and Wande Ding are the first authors.

HIGHLIGHTS

- DDBAC was used to further improve the flotation efficiency of CMP-DAF.
- The interaction force between bubbles and floc particles was greatly improved.
- The removal rate of turbidity and floc particles increased.

INTRODUCTION

Recently, with rapid economic development and population growth, water scarcity has become a key issue limiting the urbanization process worldwide, especially in northern China. To address the pressing issue of water shortage, the government of China has delivered water diversion and water transfer projects, such as the South-to-North Water Diversion, to meet the water requirements of northern China and facilitate the urbanization process (Zhao *et al.* 2017; Yu *et al.* 2018). However, the water transferred from southern China presents seasonally low temperature, low turbidity and high algae (Yu *et al.* 2018). More importantly, the number of floc particles in raw water is relatively small, and it is hardly removed by conventional flocculation and precipitation. Therefore, it is often difficult for the effluent quality to meet the drinking water standard.

A few studies have proposed that the dissolved air flotation (DAF) process can certainly improve the effluent quality to some extent (Teixeira & Rosa 2006; Edzwald 2010). However, the presence of algae in raw water, low turbidity as well as high energy consumption and low

doi: 10.2166/ws.2020.114

adhesion efficiency pose great challenges to DAF in practical use. It is urgent to improve DAF technology so that the effluent quality can reach a better level.

An effective method is the combination of a centrifugal multiphase pump (CMP) and DAF (CMP-DAF), in which CMP is utilized for air saturation and bubble generation by hydrodynamic cavitation (Pioltine & Reali 2011; Zaneti *et al.* 2013; Azevedo *et al.* 2017). The advantages of high volumetric efficiency, elimination of saturation chambers and air supplied from the atmosphere rather than from a compressor make this method one of the most promising technologies for improving the removal efficiency of DAF. Azevedo *et al.* (2017) used an EDUR®-EB3 multiphase pump for dissolved gas, demonstrating that CMP-DAF exhibits higher separation efficiency at high hydraulic loads (9–15 m/h), even without polymerization. The effluent can still reach 2 NTU (10–25 NTU raw water). Etchepare *et al.* (2017) used a Nikuni®-KTM20ND multiphase pump for gas separation. The concentration of nanobubbles measured after separation of micron-sized bubbles was as high as 1.5×10^8 cells/mL, and the average size of the nanobubbles was between 200 and 250 nm. Despite this great achievement, the same problem was also faced with CMP-DAF – low adherence of floc particles and bubbles, which blocked higher removal efficiency when treating complicated raw water.

Several studies have reported that bubble size and hydrodynamic behavior played a significant role in the formation of bubble–floc particle aggregates and thereby in the performance of flotation operation (Han 2002; Fanaie *et al.* 2019; Lee *et al.* 2019; Wang *et al.* 2019). To adjust the size of bubbles, surfactants are generally added to the treatment system, and their role in the flotation process is discussed by analyzing the surfactant effects on the bubble velocity, size, gas holdup and gas transfer rates (Hebrard *et al.* 2009; Painmanakul *et al.* 2010). Li *et al.* (2012) studied the effects of surfactant on bubble hydrodynamic behavior under flotation-related conditions in wastewater. The results showed that the addition of surfactant into pure water dampened bubble deformation, reduced bubble size and increased the specific surface area of the bubble swarm. Xia *et al.* (2009) and Wang & Ren (2005) tested quaternary ammonium salt surfactants as collectors for the flotation of silicates. The results demonstrated that quaternary ammonium salt surfactants had significant selectivity and collectability. The bubble size was effectively controlled by the addition of surfactants. The conclusions implied that the addition of surfactant not only effectively adjusted the bubble size, but also enhanced the interaction between bubbles and small suspended floc particles, thus improving the removal efficiency in the flotation process (Reis & Barrozo 2016). Nevertheless, most of the above studies focused on the effect of the addition of surfactant on the traditional DAF process and were related to bubble motion in pure water and surfactant solutions (Liao *et al.* 2004; Passos *et al.* 2015). Studies on the effect of surfactant addition on the CMP-DAF process using actual drinking water have been rare until now. This motivates the present work.

In the present study, dodecyl dimethyl benzyl ammonium chloride (DDBAC) was utilized as flotation agent to further increase the removal efficiency for different pollutants during the CMP-DAF process. First, we systematically investigated the removal rate of different pollutants before and after the addition of DDBAC. Second, the change in bubble size before and after the addition of DDBAC was studied. Finally, we analyzed the removal mechanism of DDBAC-assisted CMP-DAF (DCMP-DAF), which is shown in Figure 1.

MATERIALS AND METHODS

Raw water quality

The raw water was supplied from the Yellow River, which has operated stably for ten years. The water quality parameters are shown in Table 1.

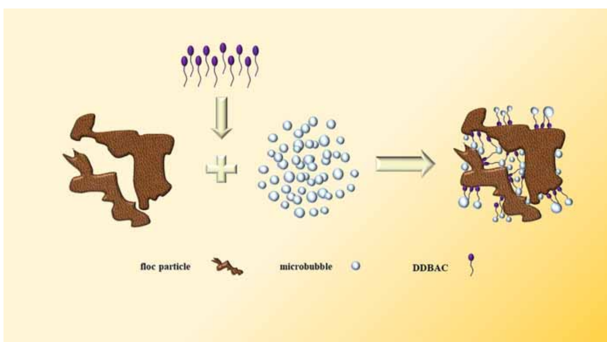

Figure 1 | Removal mechanism of DDBAC-assisted CMP-DAF.

Table 1 | Parameters of raw water quality

Item	pH	Turbidity (NTU)	TOC ($mg \cdot L^{-1}$)	COD_{Mn} ($mg \cdot L^{-1}$)	UV_{254} (cm^{-1})	Particles ($cnt \cdot mL^{-1}$)	Temperature (°C)
Value	8.11–8.38	1.92–3.35	2.983–3.633	3.10–3.25	0.050–0.052	12,835–21,568	5–10

Pilot plant and test method

The pilot-scale experiment setup ran continuously and was located at the Quehua Water Plant in Jinan, which belongs to the National Science and Technology Major Special Pilot Base. The experimental setup is shown in Figure 2. The experimental setup was composed of a mixing tank, flocculation chamber, contact zone, floating zone and tube settler. The overall size of the floating zone and the tube settler was 2.6 m × 0.8 m × 4.3 m. The test lasted for 20 days from December 20 to January 10, when the raw water was characterized by low temperature and low turbidity as shown in Table 1.

Test conditions

Design processing capacity, 10.0 m^3/h; coagulant used: PAFC, dosage [Al^{3+}], 5.0 mg/L; DDBAC, dosage, 0.2 mg/L; hydraulic load value (HL), 10.4 m/h; sampling frequency, once a day; sampling point, reflux tank.

The operating pressure, reflux ratio, and vacuum of the CMP were 0.5 MPa, 20% and −0.01 MPa, respectively.

Test process

The two chemicals (poly-aluminum-ferric chloride (PAFC), DDBAC) are added to the raw water. Then, the raw water runs through the mixing tank, flocculation chamber, and contact room and enters the floating zone. Subsequently, the water passes through the tube settler separation zone and flows into the reflux tank. Water and air are sucked into the CMP, and a uniform mixture of water and air is formed. The mixture passes through the expansion tube and is released from the gate valve in the contact chamber.

Analysis methods

Turbidity is measured by a portable turbidimeter (Hach, 2100N). The number of floc particles is determined using a benchtop particle counter. COD_{Mn} is measured by the potassium permanganate method. UV_{254} is investigated spectrophotometrically (Hach, DR5000). Total organic carbon (TOC) is determined by a Shimadzu total organic carbon analyzer (Shi-madzu, TOC-VCPH). The average bubble particle size is measured according to Stokes' theory, and calculated by Equations (1) and (2) (Ruby & Majumder 2018; Tao et al. 2019):

$$V = \frac{H}{T} \tag{1}$$

$$d = \sqrt{\frac{18\mu V}{g(\rho - \rho_g)}} \tag{2}$$

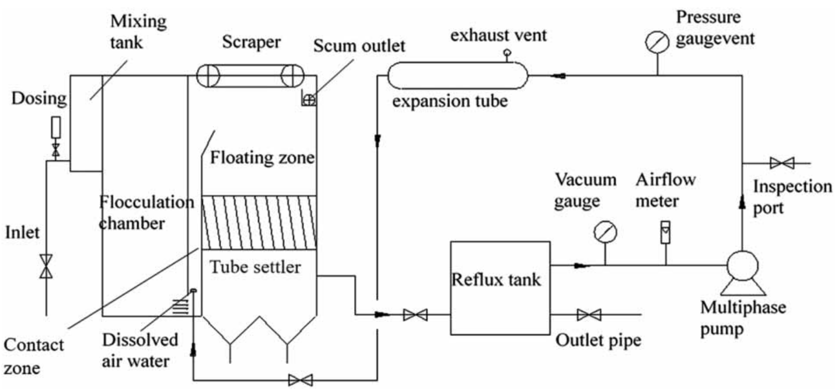

Figure 2 | Experimental setup.

where H is water height in the cylinder, T is the time that the bubble floated to the surface of the water completely, d is the diameter of the microbubble, μ is the viscosity of the liquid or slurry, V is the rise velocity of the microbubble, g is the gravitational acceleration, ρ is the density of the liquid–microbubble mixture, and ρ_g is the density of the microbubble gas.

RESULTS AND DISCUSSION

Removal efficiency of turbidity

The effluent turbidity and removal rate of CMP-DAF and DCMP-DAF are shown in Figure 3. As obtained, the effluent turbidity of CMP-DAF varied from 0.519 ± 0.026 to 0.765 ± 0.03 NTU. When 0.2 mg/L DDBAC was added to the air flotation system, the average effluent turbidity decreased from 0.608 ± 0.058 NTU to 0.433 ± 0.017 NTU. In addition, it was also found that DCMP-DAF had better control of effluent turbidity and better impact resistance to the complicated raw water, which resulted in more stable effluent turbidity. In contrast, the effluent turbidity trend of CMP-DAF corresponded to that of the raw water. When the turbidity of the raw water increased, the effluent turbidity of CMP-DAF increased and vice versa.

The difference between the effluent turbidity of CMP-DAF and DCMP-DAF was most likely induced by the addition of DDBAC. DDBAC is an amphiphilic surfactant, and its structure is shown in Figure 4(a) (Hu *et al.* 2019). When DDBAC was introduced to the emulsion, the hydrophilic groups adhered to the surface of the floc particles, and the hydrophobic groups adhered to the surface of the nanobubbles (Figure 4(b)). Since the hydrophobic group contained a polarizable aromatic ring, π-electron polarization adsorbed on the positively charged portion of the floc particle surface, and two or more floc particles were connected, forming a bridge (Wang *et al.* 2019). As a result, adhesion of the bubble to the hydrophilic floc particles was achieved, which was not easily desorbed and enhanced the air flotation efficiency. The same results were also reported by Yap *et al.* (2014), in which the removal rate of algae was higher than 95%.

Removal efficiency of floc particles

To study the change in the number of floc particles in the effluent of CMP-DAF and DCMP-DAF, 20 samples were

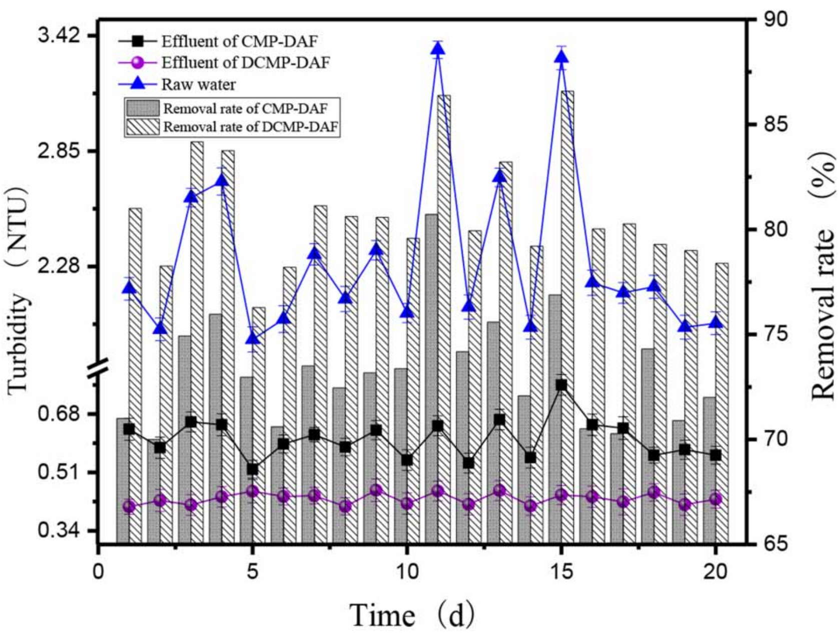

Figure 3 | Comparison of effluent turbidity and removal rates of CMP-DAF and DCMP-DAF.

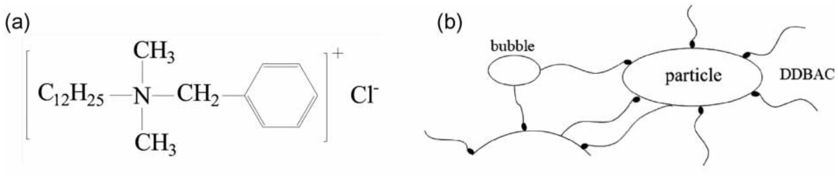

Figure 4 | (a) Structure of DDBAC and (b) diagram of the bridge between nanobubbles and floc particles.

collected and measured, and the results are displayed in Figure 5. It was obvious that both DCMP-DAF and CMP-DAF exhibited excellent separation performance (above 97%), and there was little difference regarding floc particles sized larger than 5 μm. In contrast, the number of floc particles sized smaller than 5 μm in the effluent of DCMP-DAF decreased compared with that of CMP-DAF, demonstrating that the addition of DDBAC had a better effect on the removal rate of floc particles of small size, while the strengthening effect gradually weakened as the floc particle size increased. The proportion of effluent floc particles with different sizes in DCMP-DAF is shown in Figure 5(b). Several studies have reported that the purification performance of DAF is largely determined by the adherence of floc particles and bubbles and separation occurring in the DAF separation zone (Yoon 2000; Basařová *et al.* 2017; Wang *et al.* 2019). Due to the low adherence of floc particles and bubbles, DAF had a better removal rate for large molecules and hydrophobic components than for small hydrophilic molecules.

Fortunately, DDBAC is an amphiphilic surfactant, and the addition of DDBAC in the DCMP-DAF system was conducive to enhancing the interaction between hydrophilic floc particles and bubbles, which is described in Figure 6. In addition, Féris & Rubio (1999) proposed that the addition of a flotation agent in the flotation system could reduce the size of the bubbles and increase the number of bubbles. The hydrophilic floc particles surrounded by uniform bubbles more easily floated to the water surface and were waved away by the scraper in the floating zone, thus increasing the removal rate of the small hydrophilic floc particles (Watcharasing *et al.* 2009). Furthermore, the proportion of effluent floc particles of different sizes in DCMP-DAF is shown in Figure 5(b).

Removal efficiency of organic matter

UV_{254} is an important parameter in raw water, reflecting the content of humus macromolecular organic compounds and aromatic compounds containing C = C double bonds and C = O double bonds (Wang *et al.* 2018). The low polarity of UV_{254} makes it easy to adsorb. To study the removal efficiency of UV_{254} for both CMP-DAF and DCMP-DAF, 20 effluent samples were measured and the results are displayed in Figure 7(a). During the continuous operation of CMP-DAF, the influent UV_{254} ranged from 0.050 to 0.052 cm^{-1}, and the

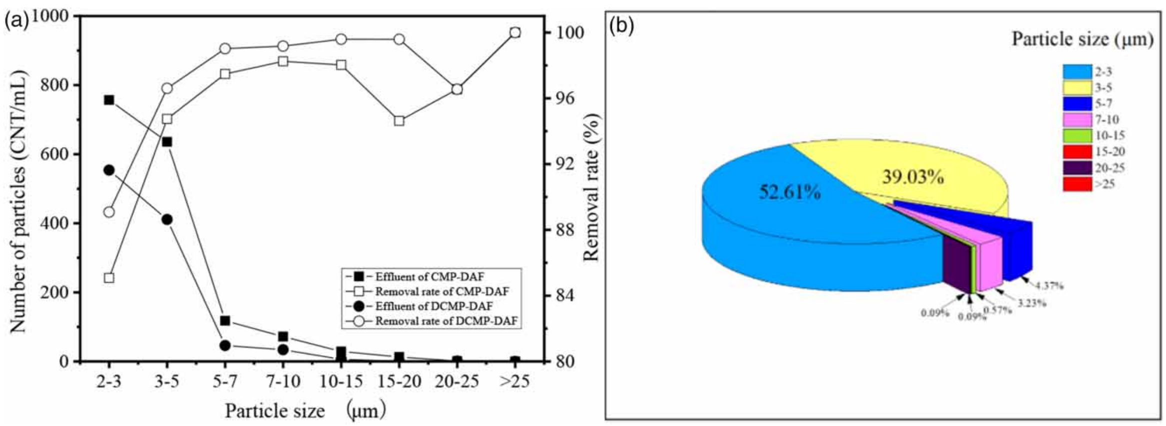

Figure 5 | (a) Comparison between the effluent floc particle numbers of CMP-DAF and DCMP-DAF, and (b) the proportion of floc particles with different sizes in DCMP-DAF.

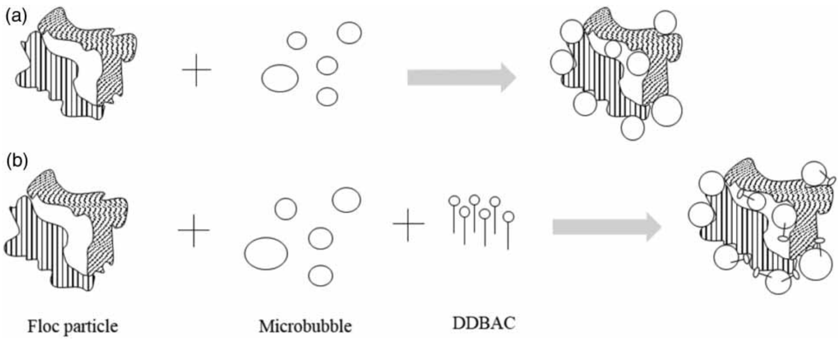

Figure 6 | Interaction between floc particles and microbubbles of (a) CMP-DAF and (b) DCMP-DAF.

CMP-DAF effluent UV_{254} was approximately 0.037 ± 0.001 cm^{-1} with an average removal rate of 27.8%. When DDBAC was added, the DCMP-DAF effluent UV_{254} showed a slight decrease from 0.037 ± 0.001 to 0.034 ± 0.001 cm^{-1}, and the removal rate increased to 33.5%.

COD_{Mn} is a common indicator to reflect the pollution of organic and inorganic oxidizable substances in water. COD_{Mn} forms flocs in the coagulation stage, and the flocs are floated and removed in the air flotation stage (Palaniandy *et al.* 2010). During the continuous operation of CMP-DAF, the influent COD_{Mn} ranged from 3.102 to 3.251 mg/L, and the CMP-DAF effluent COD_{Mn} was maintained at 2.367 ± 0.018 mg/L with an average removal rate of 25.4%. After the addition of DDBAC to the flotation system, the DCMP-DAF effluent COD_{Mn} decreased to 2.219 ± 0.011 mg/L, and the removal rate increased to 30.1% (Figure 7(b)).

Effect of DDBAC on the average particle size of bubbles

Size and shape are the two key properties of bubbles influencing the removal efficiency in the flotation system (Hassanzadeh *et al.* 2016; Gulden *et al.* 2018). In the present study, the average bubble size under different addition contents of DDBAC in the flotation system was evaluated according to Stokes' theory. The dissolved gas pressure was 0.5 MPa and the vacuum value was −0.01 MPa. The dissolved gas released was introduced into a 1 L measuring cylinder, and the time taken for a bubble to float to the surface of the water was recorded by a stopwatch. Then, the diameter of the bubbles was calculated, which is summarized in Table 2.

As obtained from Table 2, the addition of DDBAC to the system could reduce the diameter of the bubbles in the air-floating separation zone. When the concentration of

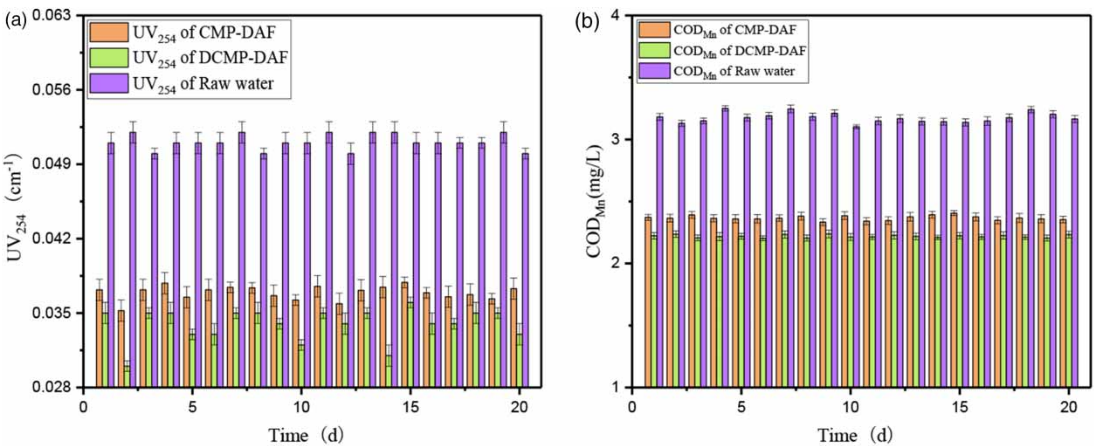

Figure 7 | (a) UV_{254} and (b) COD_{Mn} of the raw water, CMP-DAF and DCMP-DAF.

Table 2 | Average diameter of bubbles with different contents of DDBAC in the flotation system

Concentration (mg/L)	Time (s)	Height (mm)	Velocity (mm/s)	Diameter (μm)
0	354.29 ± 1.90	410	1.16 ± 0.01	46.08 ± 0.12
0.05	402.36 ± 9.11	410	1.02 ± 0.02	43.24 ± 0.49
0.1	448.62 ± 8.01	410	0.91 ± 0.02	40.95 ± 0.36
0.2	493.84 ± 10.64	410	0.83 ± 0.02	39.03 ± 0.42
0.3	494.25 ± 11.65	410	0.83 ± 0.02	39.01 ± 0.46
0.4	488.55 ± 6.47	410	0.84 ± 0.01	39.24 ± 0.26

DDBAC increased, the diameter of the bubbles decreased. When the content of DDBAC was 0.2 mg/L, the average diameter of the bubbles in DCMP-DAF was 39.03 ± 0.42 μm, which was 7.05 μm lower than that in CMP-DAF. However, it was obvious that the diameter of the bubble remained unchanged as the content of DDBAC further increased.

Rykaart & Haarhoff (1995) proposed that the bubble generation process mainly went through two stages: (1) bubbles are generated and grown on the bubble core of dissolved gas water, which is released through high pressure; (2) in the air-floating separation zone, bubbles gradually grow as they coalesce. In the general process of model calculation, certain assumptions were made. For the traditional DAF and CMP-DAF, the bubble sizes generated ranged from 30 to 100 μm, which can be simplified as a spherical shape. According to the theory of complementary nuclei, when the two phases of gas and liquid are not saturated, the saturation required to form bubbles is due to the lack of gas cavities in the solution (Xi *et al.* 2019). However, once bubbles are generated, new bubbles are hardly formed at the same position. We can calculate the critical diameter of the bubbles using the following Equation (3) (Edzwald 1995):

$$d_{cd} = \frac{4\sigma}{\Delta P} \tag{3}$$

where d_{cd} is the critical diameter of the bubble, σ is the surface tension of water, and ΔP is the pressure difference on both sides of the dissolved water releaser.

It can be seen from Equation (3) that lower surface tension of the solution and higher dissolved gas pressure may result in a smaller diameter of the bubble (Edzwald 1995). When the pressure in the multiphase pump reaches 0.4–0.6 MPa, the critical diameter of the bubble is calculated to be <1 μm according to the equation. Some scholars believe that the smaller the bubble radius is, the slower is the rise rate, which is conducive to the full adhesion of bubbles and floc particles (Sobhy & Tao 2013). However, in the actual air flotation separation process, the particle size of the bubbles adhering to the floc particles is much higher than the calculated critical value. In addition, the SM model, Gaudin model and Flint–Howarth model are three typical models of collisions between bubbles and floc in the air flotation separation zone. All three models reflect that a smaller diameter of bubbles and larger diameter of the floc particles may increase the collision efficiency between bubbles and floc particles (Ducker *et al.* 1994). As shown in Table 2, after the addition of DDBAC, the bubble diameter decreased to a certain extent, which was believed to increase the collision efficiency and improve the air flotation efficiency.

When a small amount of DDBAC was added, the surface tension of the liquid was first reduced. According to the theory of complementary nuclei, the critical diameter of the generated bubble group was reduced when bubbles precipitated at the nucleation site (Xi *et al.* 2019). Since the hydrophobic end of the DDBAC molecule was more easily bound to the bubble, a layer of DDBAC molecules was adsorbed on the surface of the bubble, which was embedded in the water film around the bubble, as shown in Figure 8(a). The van der Waals force between bubbles was weakened and the hydrodynamic repulsion was strengthened; thus, the coalescence between bubbles was weakened, and the average particle size of the bubble was reduced (Sobhy & Tao 2013). In contrast, when the concentration of DDBAC molecules in water was too high, the adhesion mode of DDBAC changed, as shown in Figure 8(b). These bubbles gathered and adsorbed to each other and then formed micelles that were stable in water. The micelles had little effect on the aggregation of bubbles, and the particle size of the bubbles remained unchanged at a certain level, which was evidenced to have a slight influence on the removal efficiency for turbidity, floc particles and organic matter (Basařová *et al.* 2017).

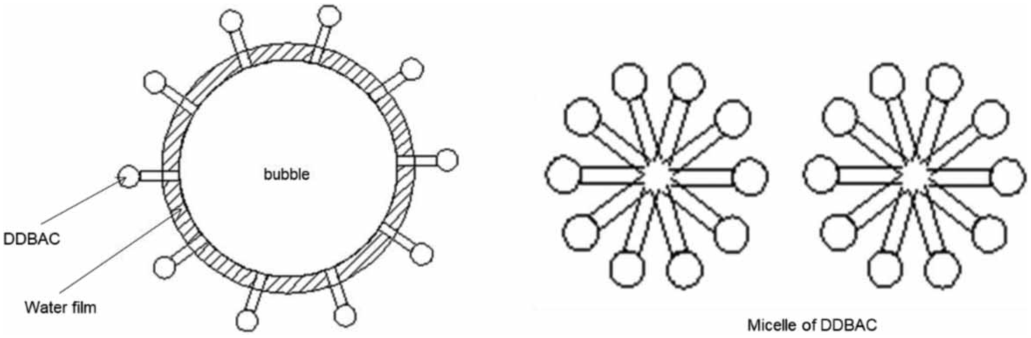

Figure 8 | Schematic diagram of the adsorption state of (a) a small amount of DDBAC and (b) a large amount of DDBAC in water.

CONCLUSION

In the present study, DDBAC was utilized as a flotation agent to enhance the adherence of floc particles and bubbles, and further improve the removal efficiency in treating low-temperature and low-turbidity water. We analyzed the effect of the flotation agent on bubble size and the possible removal mechanism of floc particles after the addition of DDBAC was also studied. The results showed that the addition of DDBAC in the flotation system performed better in removing turbidity and floc particles than UV_{254} and COD_{Mn}. The average effluent turbidity decreased from 0.608 ± 0.058 NTU to 0.433 ± 0.017 NTU with a removal rate increased by 25.8%; the removal rate of floc particles larger than 5 μm surpassed 97%, while the removal rates of UV_{254} and COD_{Mn} were increased by only 5.7% and 4.7%, respectively. In addition, the average diameter of the bubble decreased from 46.08 ± 0.12 μm in DCMP-DAF to 39.03 ± 0.42 μm in CMP-DAF, which convincingly improved the removal efficiency in the treatment of low-temperature and low-turbidity water.

ACKNOWLEDGEMENTS

This research was founded by the Major National Science and Technology Project for Water Pollution Control and Treatment (2012zx07404-003-006).

CONFLICTS OF INTEREST

The authors declare no conflict of interest.

REFERENCES

Azevedo, A., Etchepare, R. & Rubio, J. 2017 Raw water clarification by flotation with microbubbles and nanobubbles generated with a multiphase pump. *Water Science and Technology* **75** (10), 2342–2349.

Basařová, P., Suchanová, H., Soušková, K. & Váchová, T. 2017 Bubble adhesion on hydrophobic surfaces in solutions of pure and technical grade ionic surfactants. *Colloids and Surfaces A: Physicochemical and Engineering Aspects* **522**, 485–493.

Ducker, W. A., Xu, Z. G. & Israelachvili, J. N. 1994 Measurements of hydrophobic and DLVO forces in bubble–surface interactions in aqueous solutions. *Langmuir* **10** (9), 3279–3289.

Edzwald, J. K. 1995 Principles and applications of dissolved air flotation. *Water Science and Technology* **31** (3–4), 1–23.

Edzwald, J. K. 2010 Dissolved air flotation and me. *Water Research* **44** (7), 2077–2106.

Etchepare, R., Oliveira, H., Nicknig, M., Azevedo, A. & Rubio, J. 2017 Nanobubbles: generation using a multiphase pump, properties and features in flotation. *Minerals Engineering* **112**, 19–26.

Fanaie, V. R., Khiadani, M. & Ayres, T. 2019 Effects of internal geometry on hydrodynamics of dissolved air flotation (DAF) tank: an experimental study using particle image velocimetry (PIV). *Colloids and Surfaces A: Physicochemical and Engineering Aspects* **575**, 382–390.

Féris, L. A. & Rubio, J. 1999 Dissolved air flotation (DAF) performance at low saturation pressures. *Filtration & Separation* **36** (9), 61–65.

Gulden, S. J., Riedele, C., Rollié, S., Kopf, M.-H. & Nirschl, H. 2018 Online bubble size analysis in micro flotation. *Chemical Engineering Science* **185**, 168–181.

Han, M. Y. 2002 Modeling of DAF: the effect of particle and bubble characteristics. *Journal of Water Supply: Research and Technology – Aqua* **51** (1), 27–34.

Hassanzadeh, A., Hassas, B. V., Kouachi, S., Brabcova, Z. & Çelik, M. S. 2016 Effect of bubble size and velocity on collision

efficiency in chalcopyrite flotation. *Colloids and Surfaces A: Physicochemical and Engineering Aspects* **498**, 258–267.
Hebrard, G., Zeng, J. & Loubiere, K. 2009 Effect of surfactants on liquid side mass transfer coefficients: a new insight. *Chemical Engineering Journal* **148** (1), 132–138.
Hu, Y., Su, M., Xie, X., Sun, C. & Kou, J. 2019 Few-layer graphene oxide with high yield via efficient surfactant-assisted exfoliation of mildly-oxidized graphite. *Applied Surface Science* **494**, 1100–1108.
Lee, K. H., Kim, H., Kuk, J. W., Chung, J. D., Park, S. & Kwon, E. E. 2019 Micro-bubble flow simulation of dissolved air flotation process for water treatment using computational fluid dynamics technique. *Environmental Pollution* **256**, 112050.
Li, Y., Zhu, T., Liu, Y., Tian, Y. & Wang, H. 2012 Effects of surfactant on bubble hydrodynamic behavior under flotation-related conditions in wastewater. *Water Science and Technology* **65** (6), 1060–1066.
Liao, Y., Wang, J., Nunge, R. J. & McLaughlin, J. B. 2004 Comments on 'Bubble motion in aqueous surfactant solutions'. *Journal of Colloid and Interface Science* **272** (2), 498–501.
Painmanakul, P., Sastaravet, P., Lersjintanakarn, S. & Khaodhiar, S. 2010 Effect of bubble hydrodynamic and chemical dosage on treatment of oily wastewater by Induced Air Flotation (IAF) process. *Chemical Engineering Research and Design* **88** (5–6), 693–702.
Palaniandy, P., Adlan, M. N., Aziz, H. A. & Murshed, M. F. 2010 Application of dissolved air flotation (DAF) in semi-aerobic leachate treatment. *Chemical Engineering Journal* **157** (2–3), 316–322.
Passos, A. D., Voulgaropoulos, V. P., Paras, S. V. & Mouza, A. A. 2015 The effect of surfactant addition on the performance of a bubble column containing a non-Newtonian liquid. *Chemical Engineering Research and Design* **95**, 93–104.
Pioltine, A. & Reali, M. A. P. 2011 Multiphase pump as microbubble generator for flotation system applied to pre-treatment of textile wastewater. *Engenharia Sanitaria e Ambiental* **16** (2), 167–174.
Reis, A. S. & Barrozo, M. A. S. 2016 A study on bubble formation and its relation with the performance of apatite flotation. *Separation and Purification Technology* **161**, 112–120.
Ruby, K. & Majumder, S. K. 2018 Studies on stability and properties of micro and nano-particle-laden ionic microbubbles. *Powder Technology* **335**, 77–90.
Rykaart, E. M. & Haarhoff, J. 1995 Behaviour of air injection nozzles in dissolved air flotation. *Water Science and Technology* **31** (3–4), 25–35.
Sobhy, A. & Tao, D. 2013 Nanobubble column flotation of fine coal particles and associated fundamentals. *International Journal of Mineral Processing* **124**, 109–116.
Tao, X. H., Liu, Y. F., Jiang, H. & Chen, R. Z. 2019 Microbubble generation with shear flow on large-area membrane for fine particle flotation. *Chemical Engineering and Processing – Process Intensification* **145**, 107671.
Teixeira, M. R. & Rosa, M. J. 2006 Comparing dissolved air flotation and conventional sedimentation to remove cyanobacterial cells of *Microcystis aeruginosa* Part I: The key operating conditions. *Separation and Purification Technology* **52** (1), 84–94.
Wang, Y. H. & Ren, J. W. 2005 The flotation of quartz from iron minerals with a combined quaternary ammonium salt. *International Journal of Mineral Processing* **77** (2), 116–222.
Wang, Y. L., Xu, X. X., Jia, R. B., Liu, B. Z., Song, W. C. & Jia, J. Q. 2018 Experimental study on the removal of organic pollutants and NH_3-N from surface water via an integrated copolymerization air flotation–carbon sand filtration process. *Journal of Water Supply: Research and Technology – Aqua* **67** (5), 506–516.
Wang, S. W., Albijanic, B., Tao, X. X. & Fan, H. D. 2019 Thin liquid film drainage mechanism between air bubbles and low-rank coal particles in the presence of surfactant. *Fuel Processing Technology* **186**, 18–24.
Watcharasing, S., Kongkowit, W. & Chavadej, S. 2009 Motor oil removal from water by continuous froth flotation using extended surfactant: effects of air bubble parameters and surfactant concentration. *Separation and Purification Technology* **70** (2), 179–189.
Xi, X., Liu, H., Cai, C., Jia, M. & Yin, H. 2019 Analytical investigation on homogeneous nucleation of bi-component fuels. *International Journal of Heat and Mass Transfer* **132**, 498–507.
Xia, L. Y., Zhong, H., Liu, G. Y. & Wang, S. 2009 Utilization of soluble starch as a depressant for the reverse flotation of diaspore from kaolinite. *Minerals Engineering* **22** (6), 560–565.
Yap, R. K. L., Whittaker, M., Diao, M., Stuetz, R. M., Jefferson, B., Bulmus, V., Peirson, W. L., Nguyen, A. V. & Henderson, R. K. 2014 Hydrophobically-associating cationic polymers as micro-bubble surface modifiers in dissolved air flotation for cyanobacteria cell separation. *Water Research* **61**, 253–262.
Yoon, R.-H. 2000 The role of hydrodynamic and surface forces in bubble–particle interaction. *International Journal of Mineral Processing* **58** (1–4), 129–143.
Yu, M., Wang, C., Liu, Y., Olsson, G. & Wang, C. 2018 Sustainability of mega water diversion projects: experience and lessons from China. *Science of The Total Environment* **619–620**, 721–731.
Zaneti, R. N., Etchepare, R. & Rubio, J. 2013 Car wash wastewater treatment and water reuse – a case study. *Water Science and Technology* **67** (1), 82–88.
Zhao, Z.-Y., Zuo, J. & Zillante, G. 2017 Transformation of water resource management: a case study of the South-to-North Water Diversion project. *Journal of Cleaner Production* **163**, 136–145.

First received 8 October 2019; accepted in revised form 19 May 2020. Available online 29 May 2020